J Mol Model (2008) 14:1023–1033
DOI 10.1007/s00894-008-0345-5

ORIGINAL PAPER

Characterization of a candidate multi-pole molecular switch using computational techniques

Davood Farmanzadeh · Hassan Sabzyan

Received: 9 October 2007 / Accepted: 23 June 2008 / Published online: 22 July 2008

Abstract An organic molecule, designed in this study, is proposed as a candidate molecular switch and characterized using the B3LYP/6-31G* computational method. Structural and electronic properties of this molecular switch (M) and its singly charged (M^+ and M^-) species in their lowest and the first higher spin states are calculated and analyzed. Molecular volume and electronic spatial extent (ESE) of this nanoswitch undergo negligibly small changes (<2%) upon charging. Furthermore, the small difference between the calculated dipole moments of the M^+ and M^- species shows that switching between negative and positive poles does not significantly affect the charge transfer performance of this molecular switch. Natural bond orbital (NBO) and spin density distributions are also calculated and analyzed. A preliminary study on the response of the proposed molecular switch to the external electric field approves its function as a multi-pole nanoswitch controlled by a bias voltage.

Keywords B3LYP · Charge distribution · Molecular switch · Nano-electronics · Nano-switch · Spin density

Introduction

Design and production of reliable and low cost storage devices have been in order in the past five decades because of continuous increase in the amount of data which should be stored [1]. Access time, physical safety and security of the stored data, and more importantly, size of the storage devices are critical characteristics in their usage in a variety of instruments, mainly computers. Therefore, miniaturization of electronic devices and components has attracted attention of chemists, physicists and electronic and computer engineers. Previously, a top-down approach had been adopted for this miniaturization which has reached the limits of its physical capabilities (down to hundreds of nanometers). In the past ten years, chemists have developed a *bottom-up* approach to the construction of molecular-level devices and machines of nanometer size starting from molecules, and obtained remarkable improvement in ultra-small devices [2–8].

Molecular electronic device (MED) is an evolving field that hopes to overcome the limitations imposed by continuing device miniaturization in silicon technology [9] by providing possibility of much higher degree of integration [10]. Molecular switches are the active components of MEDs capable of inducing chemical and physical changes in response to external stimuli such as electric and magnetic fields, light, and biological impulses [11, 12]. Extensive efforts, most of which successful, have been put to investigate and design appropriate molecular devices, however, none of them presented a rigorous method for the precise description of the behavior of the proposed molecular device on the nano scale.

In the future of nano-electronics, we will certainly achieve the molecular integrated circuits (MIC) constructed from the nano-components such as molecular switches, molecular diodes and molecular capacitors. For this purpose, it is necessary to evaluate possible experimental approaches, and to design and theoretically assess function of the proposed molecular electronic components using cost efficient quantum computational techniques. Computational

D. Farmanzadeh · H. Sabzyan (✉)
Department of Chemistry, University of Isfahan,
Isfahan 81746-73441, I.R. Iran
e-mail: sabzyan@sci.ui.ac.ir

approaches can be used also to design and optimize experimental approaches, and to interpret the results of experimental investigations [13–15].

Use of a multi-pole molecular switch (to play the role of a transistor in the future nano-electronic circuits), instead of several dipole molecular switches, effectively reduces the size of the circuit toward miniaturization, as is the main aim of nanotechnology. Furthermore, the inter-switch interactions and interferences of a nano-electronic circuit made of such a switch are effectively reduced. This results in more predictable response behavior and a deterministic performance of the switch and the nano-electronic circuit.

The major purpose of this series of researches is to design multi-pole molecular switches and to theoretically study their structural and electrical properties, and their passive and active characteristics including electric conductivity and multi-pole function.

We suggest the following cost-efficient scheme for the design and characterization of multi-pole molecular switches with the desired behavior: i) Design of an appropriate molecular system based on the expected electronic performance and the known physicochemical characteristics of functional groups; ii) Evaluation of the fundamental molecular properties, such as appropriate geometry, HOMO-LUMO (band) gap and electric polarizability (as described in detail in the present article); iii) Evaluation of the response of the molecule to the external electric field; and iv) Evaluation of the properties of the electrode-molecule-electrode system required to simulate the performance of the switch in a real nano-electronic circuit. Any proposed molecular switch should pass these four evaluation steps consecutively in order to be accepted as an appropriate molecular switch for future nano-electronic circuits. Therefore, this work presents a methodology to filter out unsuitable proposed molecules in the first step and thus to save time in finding the molecule with the best desired behavior.

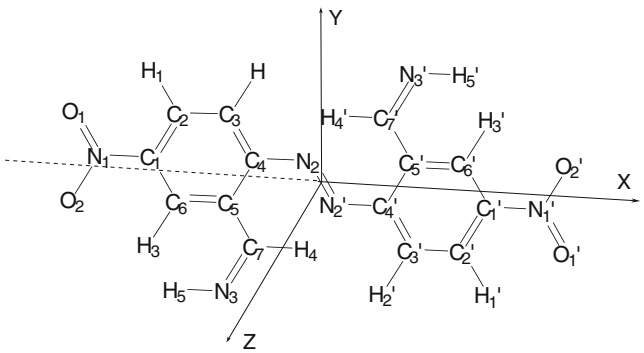

Fig. 1 Structure of the organic molecule designed and studied in this work as a multi-pole molecular switch candidate. The frame of axes used for the projection of the electric dipole moment and polarizability tensor elements is also shown

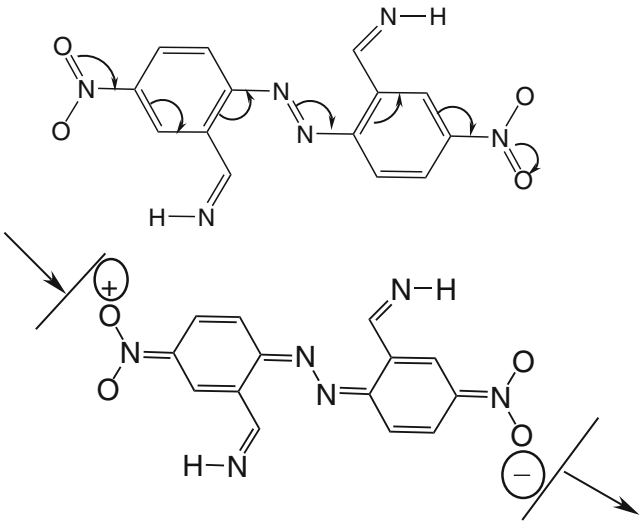

Fig. 2 Electron transfer scheme of the candidate molecular switch designed and characterized in this work. The lower structure shows the π-electrons arrangement in the turn-on position of the switch

In the present work, an organic molecule with the structure depicted in Fig. 1 is designed as a multi-pole molecular switch. Quantum chemical computational study is carried out to characterize structural and electronic properties of this molecule and to rate the possibility of its usage in nano-electronic circuits. The switching function of this molecule is triggered by the application of an electric field with a threshold strength (determined by HLG value) along the line connecting the two main (nitro) poles. The electron transfer scheme responsible for this switching is demonstrated in Fig. 2. The molecule is designed such that the threshold field strength can be adjusted and controlled by a bias voltage applied on the side chains connected to the switch via different substitutions. Therefore, it is potentially possible to turn the switch on and off also by applying appropriate bias voltages.

Computational procedures

Geometry optimization and calculation of the structural and electronic properties of the proposed molecular switch (M) and its singly charged (M^- and M^+) species have been carried out at DFT level of theory with the B3LYP gradient-corrected hybrid density functional [16, 17] using 6-31G* basis set. Gaussian G03 program package has been used throughout this work for all quantum chemical computations [18].

Thermochemical properties have been calculated for the formation reaction based on the thermochemical functions calculated for the optimized structures of the neutral molecule, the charged species, and the constituting elements in their stable forms at 298 K and 1 atm using the

same level of theory and basis set, except for those of C (graphite) which are taken from NIST [19]. Vibrational analysis required for the calculation of the thermochemical functions is carried out on the optimized structures at the same level of theory with the same basis set using a scale factor of 0.9613 recommended by Wong [20]. Analysis of the electrical properties was based on atomic electric charges and electric dipole moments and polarizability tensor elements.

In molecular electronics, devices may undergo charging and current processes. A molecular switch may be located in a positive (or negative) potential part in some instances of the function of the nano-electronic circuit, and thus as a component of that part, it may acquire positive (or negative) charge without undergoing any chemical bond breakage. Therefore, investigation of the switching between neutral and charged states is necessary. This issue is well known in biological switches [21]. Properties of both singly charged (M^- and M^+) species of the molecule are thus calculated and studied.

For molecules with extended π-systems, the higher spin levels may be located close to the ground state and may contribute to its dynamic and interactive characteristics (under static or low-frequency perturbations of the circuit fields and thermal fluctuations). In some cases, especially for those molecules having high symmetries, the high spin states may lie even lower than the low spin states and thus should be considered as the ground state. Therefore, it is necessary to investigate the higher spin states for our proposed molecular switch and its charged species to make sure that the investigated low spin state is the actual ground state. Therefore, a series of computations are carried out at the same level of theory with the same basis set on the high spin states of the neutral (triplet state) and charged species (quartet states) of the proposed multi-pole nano-switch.

Results and discussion

Structural analysis

Optimized values of some important geometric parameters are tabulated in Table 1. In this Table, and throughout this report, the numbering scheme introduced in Fig. 1 has been adopted; $R_{i,j}$ (or i-j) being the bond length between atoms i and j, and $A_{i,j,k}$ (or i-j-k) and $D_{i,j,k,l}$ (or i-j-k-l) being respectively the bond and dihedral angles formed by atoms i, j and k, and atoms i, j, k and l. As can be deduced from Table 1, the overall structure of the proposed molecular switch is not planar; while the NO_2 groups are coplanar with the benzene rings, the −CH = NH groups are slightly tilted out of the benzene rings plane. From Table 1, it can be found also that changes of the bond lengths of both benzene rings with spin multiplicity are almost identical; bond lengths such as N1-O1, N1-O2, C1-N1, and their analogs on the other side of the molecule, for all species in their high spin multiplicity states are greater than those in their corresponding low spin multiplicity states. For the low spin species, as compared with the neutral molecule, the C1-N1 and C1′-N1′ bond lengths are increased in M^+ while they are decreased in M^-. Bond lengths C4-N2 and C4′-N2′ in the neutral molecule M and its positively charged species M^+ increases with increasing spin multiplicity. This trend is reversed for the negatively charged species M^- in the corresponding spin state. For the low spin state, maximum variations caused by the positive and negative charges observed for the bond and dihedral angles is about 2.7 degrees. Changes in the bond angles in all low spin systems compared to those of the neutral molecule are lower than ±2.7 degrees, except for the changes in $A_{C4,N2,N2'}$ and $A_{C4',N2',N2}$ angles which is about 15 degrees. In comparison with other species, dihedral angles of the M^- species in its low spin state are closest to those of the neutral molecule.

Length of a molecular switch is a critical parameter characterizing its structural response to the applied external field of the nano-electronic circuit. Sensitivity of the port-to-port length of a molecular switch to the charging process can have simultaneously two opposite effects on its performance. For the cases in which the switching function is triggered by a change in the length of the molecular switch upon charging or discharging, this sensitivity is a positive feature. For the other cases in which the switching function is a consequence of a change in the dihedral angles or displacement of a moving or exchanging atom or group without altering its connections to the circuit, sensitivity of the molecular length is considered as a disadvantage of the switch. In the latter cases, the less affected the molecular length by the external field, the better the molecular switch. Therefore, it is always necessary to analyze the port-to-port length of any proposed molecular switch.

The longest inter-atomic distance O1-O1′ is assumed to represent the length, *l*, of our proposed molecular switch. The calculated values of *l* reported in Table 1 show that length of this molecular switch does not change significantly with adding a positive or negative charge; it undergoes only 0.42% and 0.50% changes, respectively. This resistance against the structural changes, while usually associated with charging of most molecules, can be considered as an advantage of the proposed molecular switch.

Another geometric parameter reflecting the global structural response of the molecular switch to the applied field is the molecular volume which is defined as the volume inside a contour of 0.001 electrons/bohr^3 density. The calculated molecular volumes with this criterion are listed in the last row of Table 1. Comparative values of the

Table 1 The optimized values of some critical bond lengths ($R_{i,j}$) in Å, and bond angles ($A_{i,j,k}$) and dihedral angles ($D_{i,j,k,l}$) in degrees, molecular length $R_{O1,O1'}$ (or *l*) in Å and molecular volume in $bohr^3 = a_0^3$, obtained at B3LYP/6-31G* level of theory for the proposed molecular switch (introduced in Fig. 1)

Prameter	M^+ (2)	M^+ (4)	M(1)	M(3)	M^-(2)	M^-(4)	M(1,1V)	M(1,10V)
$R_{C1,C2}$	1.394	1.414	1.393	1.399	1.408	1.414	1.394	1.409
$R_{C1',C2'}$	1.395	1.414	1.393	1.400	1.408	1.414	1.392	1.396
$R_{C2,C3}$	1.386	1.370	1.388	1.380	1.376	1.376	1.388	1.382
$R_{C2',C3'}$	1.386	1.370	1.388	1.380	1.376	1.377	1.389	1.386
$R_{C3,C4}$	1.413	1.434	1.404	1.420	1.425	1.422	1.405	1.429
$R_{C3',C4'}$	1.411	1.434	1.404	1.421	1.425	1.420	1.404	1.427
$R_{C4,C5}$	1.429	1.460	1.421	1.434	1.444	1.436	1.420	1.437
$R_{C4',C5'}$	1.427	1.460	1.421	1.436	1.444	1.440	1.421	1.446
$R_{C1,N1}$	1.489	1.479	1.475	1.467	1.437	1.419	1.473	1.431
$R_{C1',N1'}$	1.489	1.479	1.475	1.467	1.437	1.424	1.478	1.482
$R_{C4,N2}$	1.384	1.335	1.414	1.365	1.367	1.375	1.414	1.381
$R_{C4',N2'}$	1.384	1.335	1.414	1.364	1.367	1.375	1.413	1.372
$R_{N1,O1}$	1.224	1.226	1.229	1.231	1.244	1.262	1.231	1.262
$R_{N1',O1'}$	1.224	1.226	1.229	1.231	1.244	1.258	1.228	1.216
$R_{N1,O2}$	1.225	1.226	1.229	1.232	1.244	1.262	1.230	1.247
$R_{N1',O2'}$	1.225	1.226	1.229	1.232	1.244	1.259	1.229	1.227
$R_{O1,O1'}$ (*l*)	13.452	13.451	13.386	13.194	13.452	13.451	13.387	13.427
$A_{C4,N2,N2'}$	131.0	129.3	115.3	127.3	116.0	127.8	115.4	115.1
$A_{C4',N2',N2}$	128.9	129.4	115.3	127.9	115.9	128.4	115.2	118.3
$D_{C5,C4,N2,N2'}$	16.1	−4.0	−23.5	−8.6	−8.3	−9.9	−23.7	−15.3
$D_{C4,N2,N2'C4'}$	198.8	180.0	179.9	128.2	180.0	142.1	180.3	175.0
$D_{N2,N2',C4',C3'}$	199.0	185.8	203.1	176.1	189.5	175.3	202.7	186.6
$D_{C3,C4,C5,C7}$	180.2	173.9	173.7	177.9	173.7	177.5	174.0	174.9
$D_{C4,C5,C7,N3}$	148.2	143.5	145.7	146.3	145.7	152.8	145.6	140.4
$D_{C4',C5',C7',N3'}$	219.2	216.3	214.2	209.6	214.3	205.4	214.2	220.2
$D_{C4,C5,C7,H4}$	−32.5	−36.8	−37.7	−35.8	−37.8	−28.5	−37.7	−44.4
$D_{C4',C5',C7',H4'}$	40.4	36.5	37.5	30.9	37.8	26.1	37.6	42.2
Volume	2344.4	2386.3	2543.9	2240.2	2316.8	2296.5	2474.0	2586.1

Numbers in the parentheses in this and all other Tables denote the spin multiplicities.

molecular volume show that the changes in the molecular volume, referenced to the neutral molecule, upon charging are about −8.9% and −7.8%, respectively for the negatively and positively charged species, M^- and M^+. Because of the possibility of charge delocalization allowed by the extended π-system, such relatively large changes are not surprising. If the calculated molecular volumes are assumed to be accurate (actually, the observed variations lie within typical computational errors of ca. ~10%.), only a 9% space margin (both in 2-D and 3-D) should be considered for molecular volume variations. To avoid possible effects of inter-element interferences in the actual nano-electronic circuits containing the proposed molecular switch, clearances of several times larger than the molecular size are needed. In the meantime, these results predict that switching between positively and negatively charged states which occurs when changing polarity of the connecting poles of the nano-electronic circuit, results in only a ±(8.9−7.8)%= 1.1% change in the volume of the switch. This small change in the volume of a nano-electronic device can safely be neglected. According to a classical view, it is right that a negatively charged species should generally have larger volume than its parent neutral molecule. This, however, is not always true for molecular species that undergo structural changes. For the present case, the expected increase in the volume of the switch due to the added electron in the absence of any structural changes should be on the order of 1/166 (~+0.6%). A reduction with the same size is expected for the positively charged species. These small changes are easily buried under the typical error bars of the calculated volumes. Therefore, sources of any changes larger than these values in the molecular volume should be traced in the structural changes (mainly due to the NO_2 and −CH = NH groups; see Table 1) induced by the charging process.

Electronic and electrical properties

Electric dipole moment, electric polarizability tensor elements, electronic spatial extent (ESE), charge and spin density distributions and the gap between the highest occupied molecular orbital (HOMO) and the lowest

Table 2 Numerical values of E_{elec}, E_0, E_{HOMO}, E_{LUMO}, E_F and HLG (all in eV) of the proposed molecular switch and its singly charged species in their high and low spin states calculated at B3LYP/6-31G* level of theory

Energy	M^+ (2)	M^+ (4)	M(1)	M(3)	M^-(2)	M^-(4)	M(1,1V)	M(1,10V)
E_{elec}	−31791.97	−31790.36	−31800.27	−31799.18	−31803.04	−31800.84	−31800.27	−31801.93
E_0	−31785.49	−31783.97	−31793.73	−31792.70	−31796.54	−31794.44	−31793.73	−31793.44
$E_{HOMO}(\alpha)$	−11.24	−9.97	−7.34	−6.13	−1.65	−0.45	−7.00	−2.79
$E_{LUMO}(\alpha)$	−8.41	−6.42	−3.89	−2.86	0.28	0.33	−3.57	−1.56
$E_F(\alpha)$	−9.83	−8.20	−5.62	−4.50	−0.69	−0.06	−5.29	−2.18
$E_{HOMO}(\beta)$	−11.23	−11.17	−7.34	−7.78	−3.20	−4.07	−7.00	−2.79
$E_{LUMO}(\beta)$	−9.15	−9.91	−3.89	−4.48	−0.35	−1.33	−3.57	−1.56
$E_F(\beta)$	−10.19	−10.54	−5.62	−6.13	−1.78	−2.70	−5.29	−2.18
HLG(α-α)	2.83	3.55	3.45	3.27	1.93	0.78	3.42	1.23
HLG(α-β)	2.09	0.06	3.45	1.65	1.30	−0.88*	3.42	3.42
HLG(β-β)	2.08	1.25	3.45	3.30	2.86	2.74	3.42	3.42

*See the text for discussion on this negative value of HLG(α-β).

unoccupied molecular orbital (LUMO), or simply the HOMO-LUMO gap (HLG), are fundamental properties that have been calculated and analyzed to characterize the multi-pole nanoswitch proposed in this work. Analyses carried out on the trend of each of these electronic properties are presented in independent sections below.

HLG, Fermi level and chemical hardness

The HOMO-LUMO gap, HLG = $E_{LUMO} - E_{HOMO}$, for different spin states is calculated and analyzed as an index measuring the response to an external electric field and thus characterizing performance of the proposed nanoswitch. In an unrestricted SCF calculation different spatial orbitals are used for electrons with different spins (α and β), and therefore, three types of HLG; namely HLG(α-α), HLG(α-β) and HLG(β-β), exist which should be characterized in order to describe perfectly the band gaps structure of the system. The calculated values of E_{HOMO}, E_{LUMO} and HLG for different spinorbitals, HLG(α-α), HLG(α-β) and HLG (β-β), are reported in Table 2. This Table shows that in M^-, values of E_{HOMO} and E_{LUMO} both for α and β electrons are higher than those for the other species. It can be seen from this Table that both HOMO and LUMO energies of the α electrons in the high spin state are higher than those in the corresponding low spin state. This trend is reversed for the β electrons. From the orbital energies reported in Table 2, it can be deduced that in the more stable low spin state, charging the neutral molecule decreases the HLG value. This shows that the presence of the extra electric charge on the molecule results in more delocalization of both occupied and virtual molecular orbitals including HOMO and LUMO. It can thus be concluded that the conduction band gap of this molecular switch is decreased upon charging. Trends of the occupied and virtual orbital energies as well as the HLG values for all of the studied species in this work are visualized in Fig. 3.

As can be seen from Table 2, a negative HLG(α-β) value (−0.88 eV) is obtained for the negatively charged

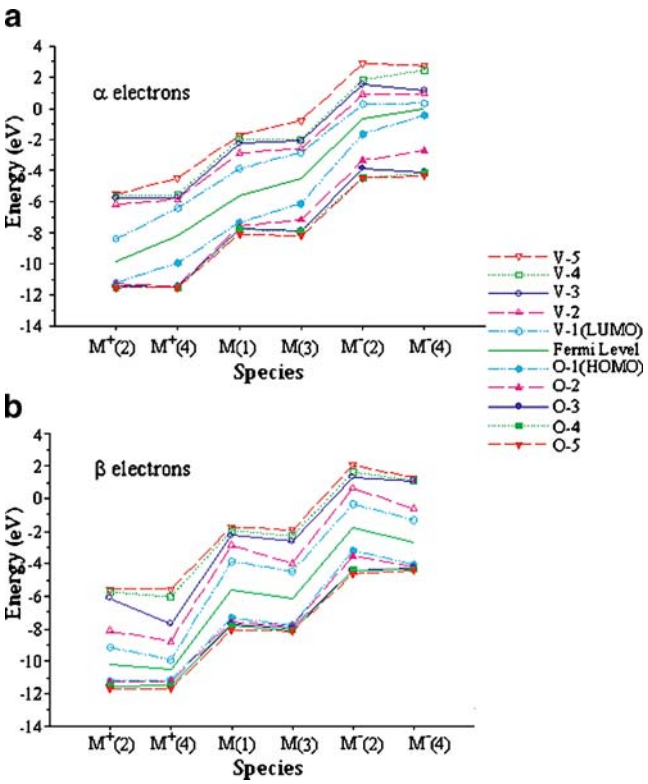

Fig. 3 Energies of the occupied (O) and virtual (V) molecular orbitals for different forms of the proposed multi-pole molecular switch calculated at DFT-B3LYP/6-31G* level of theory; (**a**) α-electrons and (**b**) β-electrons. The Fermi level located midway between the HOMO and LUMO is also drawn for comparison. Numbers in the parentheses on the labels of the horizontal axis denote the spin multiplicities. The same set of symbols is used for both parts

species in its high spin state, M^- (4). A negative value of HLG(α-β) means that the lowest virtual β state lies below the highest occupied α state. Such an occupation order arises because of imposing a high spin multiplicity (here quartet with S=3/2 for the negatively charged species) to electronic configuration in unrestricted Hartree-Fock (UHF) or Kohn-Sham open-shell calculations which requires more α (three here) than β electrons. Therefore, for systems with more than one unpaired electrons, the unrestricted calculations result in more occupied α states with unoccupied lower (available) β states. The negative HLG(α-β) value obtained for the high spin state of the negatively charged species implies that the imposed high spin multiplicity does not correspond to the lowest energy molecular state, and in spite of the lower energy of the β LUMO, two consecutive α-states are occupied. This behavior, which can be produced upon application of electric and magnetic fields, may lead to spintronics properties [22–24] and requires a thorough and independent study not intended here.

The electrical behavior of materials is largely determined by the behavior of electrons near the Fermi level (E_F). In metals, Fermi level is the energy that separates the occupied and unoccupied electron states. In common unsaturated organic molecules, the Fermi level usually lies close to the center of the HOMO-LUMO gap [25, 26]. The calculated values of the Fermi level energies for different species of the proposed molecular switch show the following order.

$$\text{Fermi Level}(E_F):\ M^-(4) > M^-(2) > M(3) > M(1) > M^+(4) > M^+(2)$$

The numbers given in parentheses here and in the rest of this article denote the spin multiplicities. This order shows that increasing spin multiplicity increases the Fermi level energy. Furthermore, charging the neutral molecule with the positive and negative charges, respectively lowers and raises the Fermi level.

Chemical hardness, developed originally as an intuitive qualitative concept, is a helpful quantity and concept to understand reactivity of a molecular system without carrying out large and long computations [27]. Chemical hardness η is commonly defined as $\eta = (I - A)/2$ in which I and A are ionization and electron affinity potentials of the species [28, 29]. This definition of chemical hardness shows that in order to calculate chemical hardness of the M^+ and M^- species, optimization and calculation of properties of the doubly charged species M^{2+} and M^{2-} are also required.

Ionization potentials (I) and electron affinities (A) were calculated (in eV) for M, M^+ and M^- species, all in their low spin states; I(M)=0.303, I(M^+)=0.447 and I(M^-)=0.103, A(M)=0.103, A(M^+)=0.303 and A(M^-)=0.025. Because of lower stability, the high spin states are not considered for the analysis of this chemical quantity. The values of the chemical hardness are then calculated (in eV) to be η(M)=2.717, η(M^+)=1.958 and η(M^-)=1.748. These values clearly show that the M^+ and M^- charged species are softer than their mother neutral molecule. Therefore, the charged states of the proposed molecular switch are overally more reactive than its neutral state. The comparative trend of the chemical hardness for neutral and charged species is consistent with what is already found from HLG values.

Electronic spatial extent (ESE)

The electronic spatial extent (ESE) for a molecule is defined as the surface area covering a volume around the molecule beyond which electron density is less than a certain value, say 0.001 electrons/bohr^3, and describing the gross receptivity of a molecule from an electric field [30]. The calculated values of ESE for the proposed molecular switch M, and its singly charged M^- and M^+ species in their high and low spin multiplicity states obtained at DFT-B3LYP/6-31G* level of theory which are reported in the lower part of Table 3, follow the order:

$$\text{ESE}: M^-(2) > M^-(4) > M^+(4) > M(1) > M^+(2) > M(3)$$

Increasing spin multiplicity for the M and M^- species decreases, while for the M^+ increases the ESE value. Comparison of the calculated ESE values shows that addition of a positive charge on the low spin neutral molecule decreases ESE values by a factor of 0.4%, while

Table 3 Numerical values of the electric dipole moment μ_t (in Debye) and diagonal elements (α_{xx}, α_{yy} and α_{zz}) and isotropic part (α_{iso}) of the electric polarizability tensor $\left(\text{in bohr}^3 = a_\circ^3\right)$ and ESE (in $a_\circ^2$) of the proposed molecular switch, and its singly charged species in their high and low spin states calculated at B3LYP/6-31G* level of theory

α_{qq}	M^+ (2)	M^+ (4)	M(1)	M(3)	M^-(2)	M^-(4)	M(1,1V)	M(1,10V)
α_{xx}	427.6	518.6	379.4	435.1	690.1	1122.7	378.9	443.7
α_{yy}	262.6	406.7	264.2	191.5	353.2	344.5	265.1	258.6
α_{zz}	116.8	76.2	78.8	154.4	79.1	147.1	78.9	90.7
α_{iso}	269.0	333.9	240.8	260.3	374.2	538.1	241.0	264.3
μ_t	21.915	21.886	0.004	3.040	21.746	21.543	1.711	23.473
ESE	24076.5	24447.5	24163.2	22992.1	24630.4	24522.8	24138.6	24115.5

Table 4 Numerical values of the natural bond orbital (NBO) atomic charges referenced to the corresponding values of the M(1) species obtained at B3LYP/6-31G* level of theory

Atom	M^+ (2)	M^+ (4)	M(1)	M(3)	M^-(2)	M^-(4)	M(1,1V)	M(1,10V)
C1	61	70	(74)	−3	−39	13	0	10
C′	59	70	(74)	−4	−39	6	0	22
C2	2	22	(−205)	−3	−21	−34	1	5
C′	3	22	(−205)	−3	−21	−40	−1	−17
C3	48	−4	(−198)	−1	−29	−13	0	4
C′	43	−4	(−198)	−4	−29	−14	0	20
C4	−43	67	(141)	−5	23	−58	1	11
C′	−38	67	(141)	−10	23	−61	−1	−4
C5	38	33	(−95)	−15	−45	−30	0	4
C′	38	34	(−95)	−19	−45	−35	1	12
C6	4	−5	(−195)	4	−3	−26	0	1
C′	2	−5	(−195)	6	−3	−10	−1	−12
C7	−35	−31	(88)	−12	16	1	0	2
C′	−37	−31	(88)	−16	16	−6	0	−3
N1	−4	−11	(513)	−5	−25	−87	−1	−28
N′	−4	−11	(513)	−5	−25	−78	1	5
N2	195	103	(−170)	44	−120	45	−1	−21
N′	191	103	(−170)	53	−120	50	0	−23
N3	82	97	(−603)	20	−52	−18	0	−7
N′	81	97	(−603)	16	−52	−25	0	7
O1	41	38	(−372)	−6	−69	−117	−1	−13
O′	40	38	(−372)	−6	−69	−107	1	14
O2	35	32	(−373)	−8	−67	−116	0	2
O′	35	32	(−373)	−8	−67	−108	0	3
H1	24	24	(280)	0	−21	−16	0	3
H′	24	24	(280)	1	−21	−16	0	−4
H2	16	14	(268)	−6	−18	−25	0	−3
H′	13	14	(268)	−3	−19	−21	0	2
H3	19	20	(278)	−1	−18	−17	0	1
H′	21	20	(278)	−2	−18	−17	0	−3
H4	4	11	(221)	−3	2	−6	0	4
H′	4	11	(221)	3	1	−3	0	7
H5	18	20	(348)	2	−13	−5	0	1
H′	19	20	(348)	1	−13	−7	0	0

Differential atomic charges ($\Delta q_A = q_A - q_A^\circ$, with q_A° being the corresponding atomic charge in M(1)) are multiplied by 1000 for simplicity. Numbers given in parentheses for M(1) are the reference NBO charges of the atoms of M(1).

addition of a negative charge increases the ESE values by 1.9%. From these comparative trends, one can conclude that this proposed molecular switch undergoes negligibly small changes in its spatial extent upon charging. This is a positive index for being used as a nanoswitch. This trend of ESE together with the trend found for molecular volumes show that charging process results in small changes in the shape of the electron density distribution toward a sphere (which has the largest volume/area ratio).

Electric dipole moment and polarizability

It has already been discussed that the size and direction of the electric dipole moment vector and values of the electric polarizability tensor elements of a molecule are the physical quantities characterizing the response of a molecule to an external electric field [30–32]. The calculated values of the size of the electric dipole moment vector $\mu_{tot.}$ (in Debye) and diagonal components (α_{xx}, α_{yy}, α_{zz}) and isotropic part (α_{iso}) of the electric polarizability tensor (in $a_\circ^3$) are listed in Table 3. Since the designed molecular switch is intended to be connected primarily via its $-NO_2$ groups, the frame of reference set such that these groups are located along the x axis; the reference frame of axes of the molecule is introduced in Fig. 1. It is obvious that the *x* component of the electric dipole moment vector (μ_x) should be the major component and thus dominantly determine the value and direction of the total electric dipole moment vector. Moreover, α_{xx} is the primary characterizing component of the polarizability tensor, and α_{yy} is thus its next important

component. It can be seen from Table 3 that the α_{xx} values for both high and low spin states of all species has the order $M^- > M^+ > M$ and for all species increases with spin multiplicity compatible with the trend found for the chemical hardness. The α_{yy} values follow the orders $M^- > M > M^+$ and $M^+ > M^- > M$ for the low and high spin multiplicity states, respectively. The polarizability data in Table 3 shows also that variations of α_{xx} and α_{iso} are correlated (because α_{xx} has the major contribution to the α_{iso}), and both increase upon charging the neutral molecule. For both spin states, α_{iso} follows thus the same order as α_{xx}, that is $M^- > M^+ > M$.

The small (less than 2%) difference between the calculated size of the dipole moment vectors of the M^+ and M^- species (21.915 D and 21.746 D, respectively) shows that the molecule is polarized almost equally upon charging with positive or negative charges. Furthermore, switching between negative and positive poles does not significantly affect the charge transfer performance of the molecular switch and its global dipolar interaction with its environment.

Charge and spin density distribution

Distribution patterns of the natural bond orbital (NBO) [33] and Mulliken [34] atomic charges have been analyzed in order to study the mutual effects of the induced charges of the substitution groups and the added electrical charges [35, 36]. Although the absolute values of the Mulliken atomic charges are different from those of NBO, they show the same trend observed for the NBO charges. Since NBO charges are superior to the Mulliken charges in that they are less sensitive to the basis set used [37], they are considered for further analysis, and therefore, the Mulliken data are not reported here for brevity. The comparative NBO charges on the nitrogen, oxygen and carbon atoms, referenced to those of the M(1) species, are reported in Table 4 and visualized in Figs. 4a and b.

The calculated NBO electric charge distribution (Table 4; Fig. 4) shows that in the neutral molecule, the largest positive charges are located on the N1 and N1′ atoms and the largest negative charges are located on the N3, N3′ and the oxygen atoms. In comparison with the neutral molecule, positive charges on the N1 and N1′ atoms in the M^+ species are increased and the negative charges on the N3, N3′ and oxygen atoms are decreased. A reverse trend is observed for the M^-.

The correspondence between the map of differential atomic charges (referenced to the neutral molecule) and the map of the spin densities in the open shell charged species imply that the added charge (via the remaining or the incoming unpaired electron) has not significantly changed the bonding structure and atomic orbital populations of the

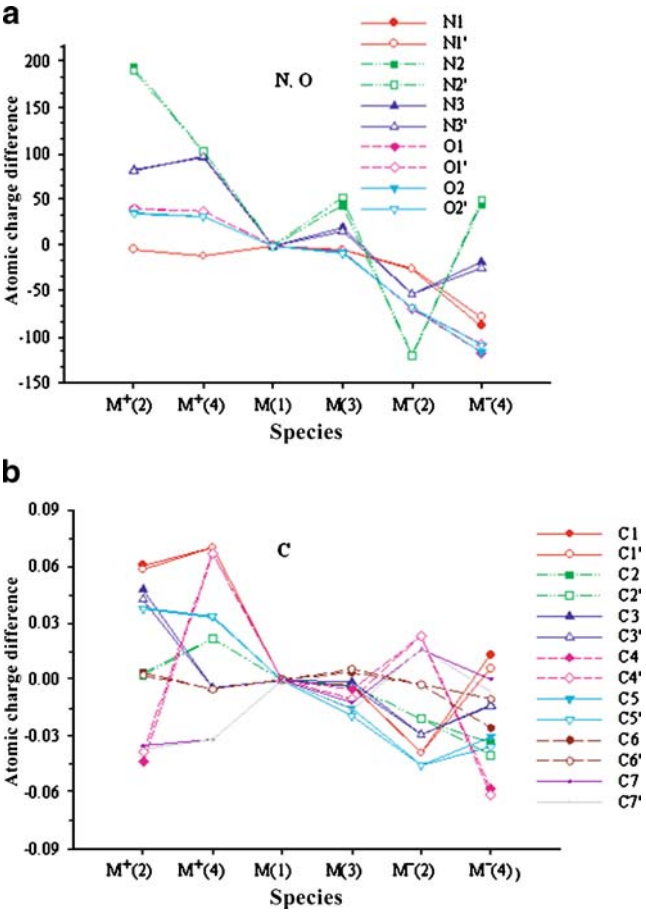

Fig. 4 Natural bond orbital (NBO) charges on the nitrogen and oxygen atoms (**a**) and carbon atoms (**b**) for different species, referenced to those of M(1) calculated for the proposed multi-pole molecular switch using DFT-B3LYP/6-31G8* method

molecule. Any noticeable mismatch between these two maps denotes a change in the bonding structure and population of the electron at one, two or more bond centers, depending on the extent of the mismatch. Analysis of the spin density distribution for the optimized structures of the open shell positively and negatively charged species of the proposed molecular switch calculated with UB3LYP/6-31G* method and reported in Table 5 shows that the map of the spin density for the open shell charged species in their low spin stable states matches with the map of differential atomic charges with some small deviations for the C4, C4′, C7′ and N3′ atoms. As a general trend, the N2 and N2′ atoms carry the largest portion of the spin density; 74% and 37% in the positively and negatively charged species, respectively.

The collective spin densities of the groups of atoms, e.g., C1-C6, C1′-C6′, NO_2 and $(NO_2)'$ are calculated and analyzed. An overview of these group spin densities shows that the spin density on the C1-C6, C1′-C6′, O1-O2, O1′-O2′, NO_2 and $(NO_2)'$ groups in M^+ species are larger than

Table 5 Numerical values of the relative (percent) spin densities distributed over the atoms in the optimized structures of the proposed molecular switch and its singly charged species[a,b] in two spin states obtained at B3LYP/6-31G* level of theory

Atom	M^+ (2)	M^+ (4)	M(3)	M^-(2)	M^-(4)
C1	5	11	9(184)	10	6
C′	5	11	9(184)	10	6
C2	−2	−3	−5(−95)	0	0
C2′	−3	−3	−5(−91)	0	1
C3	4	5	9(181)	6	4
C′	4	5	9(177)	6	3
C4	0	1	−6(−122)	−1	1
C′	0	1	−6(−119)	−1	1
C5	5	11	10(198)	9	4
C′	6	11	10(203)	9	5
C6	−2	−5	−5(−102)	−4	0
C′	−2	−5	−5(−103)	−4	−1
C7	1	−3	−3(−51)	−1	−1
C′	−4	−3	−2(−34)	−1	−1
N1	0	−1	−1(−14)	2	3
N′	0	−1	−1(−14)	2	3
N2	37	25	34(680)	18	22
N′	37	25	34(680)	19	22
N3	0	6	4(87)	2	2
N′	8	6	3(66)	2	2
O1	0	1	1(23)	5	4
O′	0	1	1(23)	4	4
O2	0	1	1(28)	5	5
O′	0	1	1(28)	5	4
H1	0	0	0(3)	0	0
H′	0	0	0(3)	0	0
H2	0	0	0(−6)	0	0
H′	0	0	0(−6)	0	0
H3	0	0	0(5)	0	0
H′	0	0	0(5)	0	0
H4	0	0	0(2)	0	0
H′	0	0	0(0)	0	0
H5	0	0	0(−2)	0	0
H′	0	0	0(−1)	0	0
Sum	100	100	100	100	100

[a] Obviously, spin density distribution is not defined for the closed shell neutral molecule.
[b] Negative spin density denotes the corresponding spin density of the unpaired β electrons.
Numbers in the parentheses under the M(3) column denote the values of the optimized spin density of M(3) multiplied by 1000.

those in M^- species. These comparative trends are the same as what is found for the collective differential NBO and Mulliken charges of the same groups of atoms. The C1-C6 and C1′-C6′ groups of atoms are the next spin populated centers of the open shell species. The collective spin densities of the NO_2 and $(NO_2)'$ groups in the $M^+(2)$ species are negligible (~0%) in comparison with those in $M^-(2)$ species (12% and 11%). The spin densities distributed over the two C7=N3 and C7′=N3′ groups of atoms in the $M^-(2)$ are equal (1%), while in $M^+(2)$ they are different (1% and 4%, respectively).

In the high spin neutral molecule M(3), the major part (68%) of the spin density is distributed over the N2 and N2′ atoms. This large inhomogeneous spin distribution shows that the atomic orbitals of these two atoms have the dominant population in the one-electron orbitals of the two unpaired electrons of the S=1 state.

The spin density maps for the open shell positively and negatively charged species in their high spin states does not exactly match the map of differential NBO and Mulliken atomic charges. It can thus be concluded that the bonding structures of these species in their higher spin states are significantly altered as compared to the mother molecule.

The spin-pairing energy for each species can be obtained by subtracting energies (E_{elec} or E_0) of the low-spin and high-spin states of that species given in Table 2. As the

energy data reported in Table 2 show, the spin-pairing energy follows the order $M^- > M^+ > M$.

Preliminary study of the field effect

In order to investigate the behavior of the molecular switch proposed in this work as an active device in a nano-electronic circuit, geometry optimization was carried out in the presence of external electric field of 1 and 10 V applied on the poles of the molecule in the x direction, passing through N1′ and N1 atoms (Fig. 1), included explicitly in the Hamiltonian of the DFT-B3LYP/6-31G* method. These fields are equivalent to 0.836 and 8.36 V/nm field strength applied over the length of molecule from N1 to N1′. The important features of the field effects on the calculated molecular properties are presented in Tables 1, 2, 3, 4 and 5. The field effect data show that the thermodynamic formation functions are not affected significantly by the applied field. A comparative analysis of the E_{elec} data (Table 2) shows that the electronic stability increases with increasing strength of the applied field. Table 2 shows that the applied field changes both HOMO and LUMO levels in a way such that the HLG values decrease in the presence of the electric field. The Fermi level energy increases with increasing strength of the applied field. The ESE values listed in Table 3, shows a small decreasing trend in the presence of electric field (only 0.1% at 1 V and 0.2% at 10 V). With these negligible changes in the ESE values, we are allowed to assume that the molecular gross receptivity is not changed under the influence of the applied field in this range of field strengths. Electric dipole moment shows a significant change in the presence of the external electric field which is quit natural for a molecule with extended π-system. Redistribution of the electric charge density under the applied electric field as shown in Table 4 approves the multi-pole function of the switch controlled by a bias voltage applied along N_3-N_3′ direction. A complete field effect study carried out on this molecular switch is reported elsewhere [38].

Conclusions

DFT-B3LYP method has been used successfully to calculate molecular properties of neutral and charged forms of the proposed molecular switch and to predict its electrical behavior and multi-pole function in an explicit external electric field. The overall structure of the switch is non-planar at the sites of the −CH = NH groups. For the case of 3D memory devices and 3D nano-circuit switches [39–41], the non-planar structure might be favored and thus becomes a positive index. To modify structural feature and field behavior of the proposed molecular switch, the −CH = NH groups can be substituted by other symmetric or asymmetric pairs of substitutions that go co-planar or out-of-plane with the other parts of the switch. The length, ESE and volume of the proposed molecule do not significantly change with charging the molecule. Equality of the lengths and dipole moments of the positively and negatively charged forms of the proposed multi-pole molecular switch denotes that its performance is not altered by switching between positive and negative potentials. The next step of this work is to study characteristics and performance of this candidate molecular switch in the presence of the polarizable poles such as small clusters of Au [42] or other types of molecular devices of the nano-electronic circuit of interest.

The methodology presented and used in this study for the characterization of a proposed molecular switch can be used in the study and prediction of the properties of any other candidate molecular devices designed for nano-electronic circuits.

Acknowledgements We would like to thank the University of Isfahan for research facilities and the University of Mazandaran and the Ministry of Science, Research and Technology (MSRT) of the Islamic Republic of Iran for financial supports as scholarship granted to D.F.

References

1. Feringa BL (2001) Molecular switches. Wiley, Weinheim
2. Balzani V, Credi A, Vanturi M (2003) Molecular devices and machines - a journey into the Nano. Wiley, Weinheim
3. Lang ND, Avouris Ph (2001) Phys Rev B 64:125323(1–7)
4. Yang Z, Lang ND, diVentra M (2003) Appl Phys Lett 82:1938–1940
5. Colton RJJ (2004) Vac Sci Technol B 22:1609–1635
6. Xue Y, Ratner MA (2004) Phys Rev B 69:085403(1–5)
7. Zhang C, Du MH, Cheng HP, Zhang XG, Roitberg AE, Krause JL (2004) Phys Rev Lett 92:158301(1–4)
8. Evers F, Weigend F, Koentopp M (2004) Phys Rev B 69:235411 (1–9)
9. Dholaki GR, Fan W, Koehne J, Han J, Meyyappan M (2004) Phys Rev B 69:153402(1–4)
10. Ernzerhof M, Zhuang M (2003) J Chem Phys 119:4134–4140
11. Loppacher C, Guggisberg M, Pfeiffer O, Meyer E, Bammerlin M, Lüthi R, Schlittler R, Gimzewski JK, Tang H, Joachim C (2003) Phys Rev Lett 90:066107(1–4)
12. Emberly EG, Kirczenow G (2003) Phys Rev Lett 91:188301(1–4)
13. Moresco F, Gourdon A (2005) Proc Natl Acad Sci USA 102:8809–88014
14. Kim YH, Jang SS, Jang YH, Goddard WA (2005) Phys Rev Lett 94:156801(1–4)
15. Lu X, Grobis M, Khoo KH, Louie SG, Crommie MF (2004) Phys Rev B 70:115418(1–8)
16. Becke AD (1993) J Chem Phys 98:5648–5652
17. Lee CT, Yang WT, Parr RG (1988) Phys Rev B 37:785–789
18. Frisch MJ, Trucks GW, Schlegel HB, Scuseria GE, Robb MA, Cheeseman JR, Montgomery Jr JA, Vreven T, Kudin KN, Burant JC, Millam JM, Iyengar SS, Tomasi J, Barone V, Mennucci B, Cossi M, Scalmani G, Rega N, Petersson GA, Nakatsuji H, Hada

M, Ehara M, Toyota K, Fukuda R, Hasegawa J, Ishida M, Nakajima T, Honda Y, Kitao O, Nakai H, Klene M, Li X, Knox JE, Hratchian HP, Cross JB, Adamo C, Jaramillo J, Gomperts R, Stratmann RE, Yazyev O, Austin AJ, Cammi R, Pomelli C, Ochterski JW, Ayala PY, Morokuma K, Voth GA, Salvador P, Dannenberg JJ, Zakrzewski VG, Dapprich S, Daniels AD, Strain MC, Farkas O, Malick DK, Rabuck AD, Raghavachari K, Foresman JB, Ortiz JV, Cui Q, Baboul AG, Clifford S, Cioslowski J, Stefanov BB, Liu G, Liashenko A, Piskorz P, Komaromi I, Martin RL, Fox DJ, Keith T, Al-Laham MA, Peng CY, Nanayakkara A, Challacombe M, Gill PMW, Johnson B, Chen W, Wong MW, Gonzalez C, Pople JA (2003) Gaussian 03. Pittsburgh PA, Gaussian Inc

19. Taken from the NIST official website at http://webbook.nist.gov/chemistry/
20. Wong MW (1996) Chem Phys Lett 256:391–399
21. Frank RAW, Titman CM, Pratap JV, Luisi BF, Perham RN (2004) Science 29 306:872–876
22. Sarma SD (2001) American Scientist 89:516–528
23. Žutić I, Fabian J, Sarma SD (2004) Rev Mod Phys 76:323–410
24. Cerletti V, Coish WA, Gywat O, Loss D (2005) Nanotech 16: R27–R49
25. Samanta MP, Tian W, Datta S, Henderson JI, Kubiak CP (1996) Phys Rev B 53:R7626–R7629
26. Datta S, Janes DB, Andres RP, Kubiak CP, Reifenberger RG (1998) Semicond Sci Technol 13:1347–1353
27. Pearson RG (2005) J Chem Sci 117:369–377
28. Tozer DJ, Proft FD (2005) J Phys Chem A 109:8923–8929
29. Pearson RG (1997) Chemical hardness. Wiley, New York
30. Sabzyan H, Omrani A (2003) J Phys Chem A 107:6476–6482
31. Sabzyan H, Mohammadi F (2004) Chem Phys 301:141–152
32. Sabzyan H, Nikoofard H (2004) Chem Phys 306:105–113
33. Reed AE, Weinstock RB, Weinhold F (1985) J Chem Phys 83:735–746
34. Mulliken RS (1955) J Chem Phys 23:1833–1840
35. Glendening ED, Reed AE, Carpenter JE, Weinhold F, NBO Version 3.1
36. Visit the NBO website at http://www.chem.wisc.edu/×nbo5/
37. Basch H, Ratner MA (2003) J Chem Phys 119:11926–11942
38. Sabzyan H, Farmanzadeh D (2007) J Computational Chem 28:922–931
39. Abe K, Fujita S, Lee TH (2005) NSTI-Nanotech 3:203, visit also the NSTI official website at http://www.nsti.org/
40. Li F, Yang X, Meeks AT, Shearer JT, Le KY (2004) IEEE Trans Device Mater Reliabil 4:415
41. Burr GW (2003) SPIE Conference on Nano- and Micro-Optics for Information Systems, Paper 5225-16
42. Jalili S, Rafii-Tabar H (2005) Phys Rev B 71:165410(1–9)